# Supporting information

## 1 General characterization

UV-vis absorption spectra were measured on a UV-2600 UV-vis spectrophotometer (Shimadzu, Japan). Grazing incidence wide-angle X-ray scattering (GIWAXS) measurements were conducted on an Xenocs-SAXS/WAXS system with an X-ray wavelength of 1.5418 Å and 0.2° as an incidence angle. Pilatus 300 K was used as a 2D detector. AFM was performed on a Bruker Dimension icon using tapping mode. The *J*−*V* curves were measured by using a Keithley 2450 SourceMeter in the nitrogen-filled glove box along the forward scan direction from −0.2 V to 1 V at room temperature. The scan speed and dwell times were fixed at 0.02 V per step and 0 ms, respectively. The photocurrent was measured under AM 1.5G illumination at 100 mW/cm$^2$ by using a 3 A solar simulator (LSS-55, Lightsky Technology Co., Ltd). Light intensity was calibrated with a standard photovoltaic cell equipped with a KG2 filter (certificated by the National Institute of Metrology). The EQE measurement was carried out in the air with a solar cell spectral response measurement system (LST-QE, Lightsky Technology Co., Ltd.). The light intensity at each wavelength was calibrated by a standard single-crystal Si photovoltaic cell. Transient photo current (TPC) and Transient photo voltage (TPV) measurements were conducted on an all-in-one characterization platform, Paios(Fluxim AG, Switzerland). In the TPV measurement, the light intensities are 0.10%, 0.23%, 0.53%, 1.23%, 2.83%, 6.52%, 15.0%, 34.6% and 80.0%, respectively, relative intensity is 20.0% and settling time is 30.0 ms, pulse length is 5.0 ms, and the follow-up time is 30.0 μs.

## 2 Chemical structure

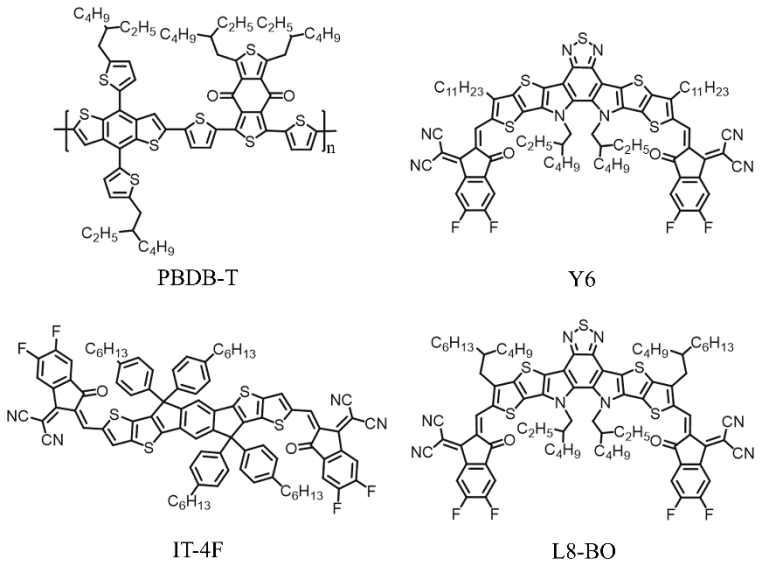


**Scheme S1** Chemical structures of PBDB-T, Y6, IT-4F and L8-BO

## 3 GIWAXS

**Table S1** The *d*-spacing and corresponding crystal coherence length (CCL) of π-π and lamellar stacking of PM6, PM6+, PM6:BTP-eC9 and PM6:BTP-eC9+ thin films

| Film | $q_z$/Å$^{-1}$ | *d*-spacing/Å | FWHM$_{\pi-\pi}$/Å$^{-1}$ | CCL$_{\pi-\pi}$/Å | $q_{xy}$/Å$^{-1}$ | *d*-spacing/Å | FWHM$_{lam}$/Å$^{-1}$ | CCL$_{lam}$/Å |
|---|---|---|---|---|---|---|---|---|
| PM6 | 1.68 | 3.74 | 0.41 | 14 | 0.29 | 21.67 | 0.097 | 58 |
| PM6+ | 1.68 | 3.74 | 0.39 | 15 | 0.30 | 20.94 | 0.092 | 62 |
| PM6:BTP-eC9 | 1.73 | 3.63 | 0.26 | 22 | 0.29 | 21.67 | 0.081 | 70 |
| PM6:BTP-eC9+ | 1.73 | 3.63 | 0.23 | 25 | 0.30 | 20.94 | 0.078 | 73 |

## 4 AFM

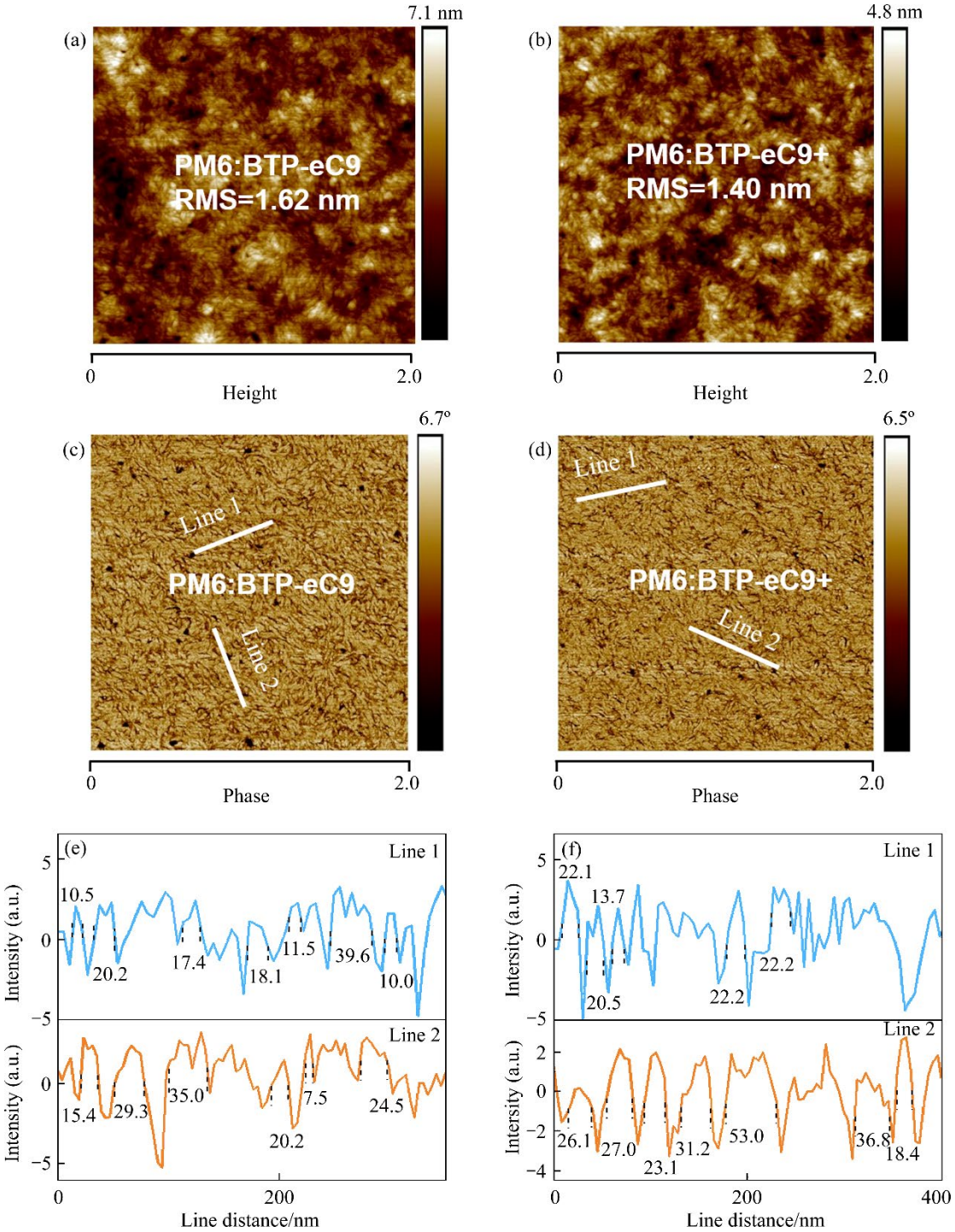


**Figure S1** AFM height images of (a) PM6:BTP-eC9 and (b) PM6:BTP-eC9+ blend films; AFM phase images of (c) PM6:BTP-eC9 and (d) PM6:BTP-eC9+ blend films; The line profiles along the white lines to obtain the nano-grain size of (e) PM6:BTP-eC9 and (f) PM6:BTP-eC9+ blend films (The nano-grain size is obtained from the average FWHMs (the distance between two adjacent dashed lines in the graph))

## 5 Impedance spectra

**Table S2** Components of the equivalent circuit as extracted by fitting the Nyquist plot data of PM6:BTP-eC9 and PM6:BTP-eC9+ based devices

| Device | $R_s$/Ω | $R_{sh}$/Ω | Impedance frequency/Hz | $\tau$/μs |
|---|---|---|---|---|
| PM6:BTP-eC9 | 43.48 | 2487 | $4.64 \times 10^4$ | 21.6 |
| PM6:BTP-eC9+ | 13.77 | 7308 | $1.47 \times 10^4$ | 68.0 |

## 6 SCLC

Charge carrier mobility was obtained by using the SCLC method. The mobility was determined by fitting the dark current to the model of a single carrier SCLC, which can be described as:

$$J = \frac{9}{8}\varepsilon_0\varepsilon_r\mu\frac{V^2}{d^3} \quad \text{(S1)}$$

where $J$ is the current density; $\mu$ is the zero-field mobility of electron ($\mu_e$) or hole ($\mu_h$); $\varepsilon_0$ is the permittivity of the vacuum; $\varepsilon_r$ is the relative permittivity of the material; $d$ is the thickness of the blend film; and $V$ is the effective voltage, $V=V_{appl}-V_{bi}$, where $V_{appl}$ is the applied voltage, and $V_{bi}$ is the built-in potential determined by the electrode work function difference.

### 6.1 Electron-only devices

The structure of electron-only devices is ITO/ZnO/active layer/Ca/Al. The ZnO precursor was spin-coated onto the ITO glass and annealed under 200 °C in air for 30 min. The PM6:BTP-eC9 blend in chlorobenzene (D:A ratio=1:1.2 (*w*/*w*)) with/without AN, was deposited onto the ZnO layer via spin-coating with 1200 r/min for 60 s. Then the film was annealed under 100 ℃ in $N_2$ for 10 min. Ca (~15 nm) and Al (~60 nm) were successively evaporated onto the active layer through a shadow mask (pressure ca. $10^{-4}$ Pa).

### 6.2 Hole-only devices

The structure of hole-only devices is ITO/PEDOT:PSS/active layer/$MoO_3$/Ag. A ~30 nm thick PEDOT:PSS layer was made via spin-coating an aqueous dispersion of PEDOT:PSS onto the ITO glass with 4000 rpm for 30 s. The PEDOT:PSS substrate was dried at 150 °C for 10 min. The PM6:BTP-eC9 blend in chlorobenzene (D:A ratio=1:1.2 (*w*/*w*)) with/without AN, was deposited onto the PEDOT:PSS layer via spin-coating with 3000 r/min for 30 s in $N_2$. Then the film was annealed under 100 °C for 10 min in $N_2$. Finally, $MoO_3$ (~3 nm) and Al (~100 nm) was successively evaporated onto the active layer under a shadow mask (pressure ca. $10^{-4}$ Pa).

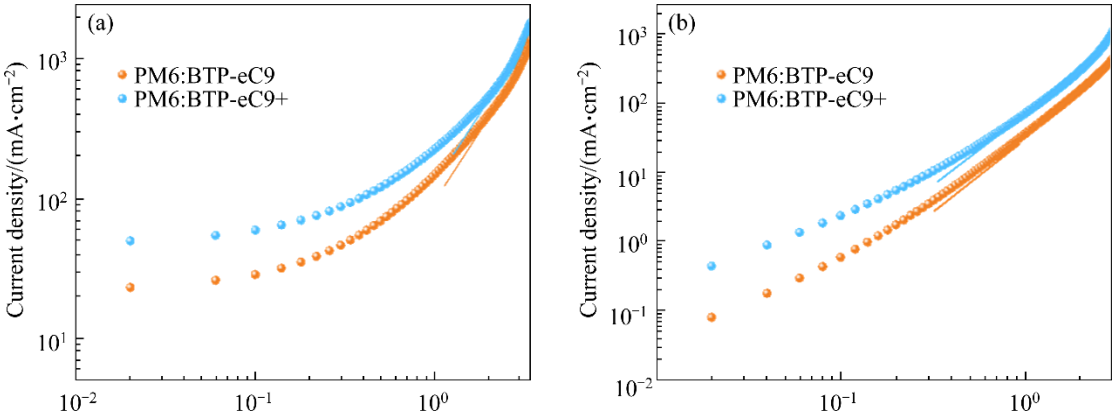


**Figure S2** Typical current density-applied voltage log plots for (a) electron-only devices and (b) hole-only devices based on PM6:BTP-eC9 and PM6:BTP-eC9+ blend films under dark. The measured data are shown as symbols, while the solid lines are the best fits to the SCLC model. Mobilities were extracted from the fitting

**Table S3** Charge carrier mobilities of devices based on PM6:BTP-eC9 and PM6:BTP-eC9+ blend films

| Blend flim | $\mu_e$/($10^{-4}$ cm$^2$·V$^{-1}$·s$^{-1}$) | $\mu_h$/($10^{-4}$ cm$^2$·V$^{-1}$·s$^{-1}$) |
|---|---|---|
| PM6:BTP-eC9 | 9.80 | 4.97 |
| PM6:BTP-eC9+ | 13.22 | 9.70 |

## 7 Photovoltaic performance of OSCs

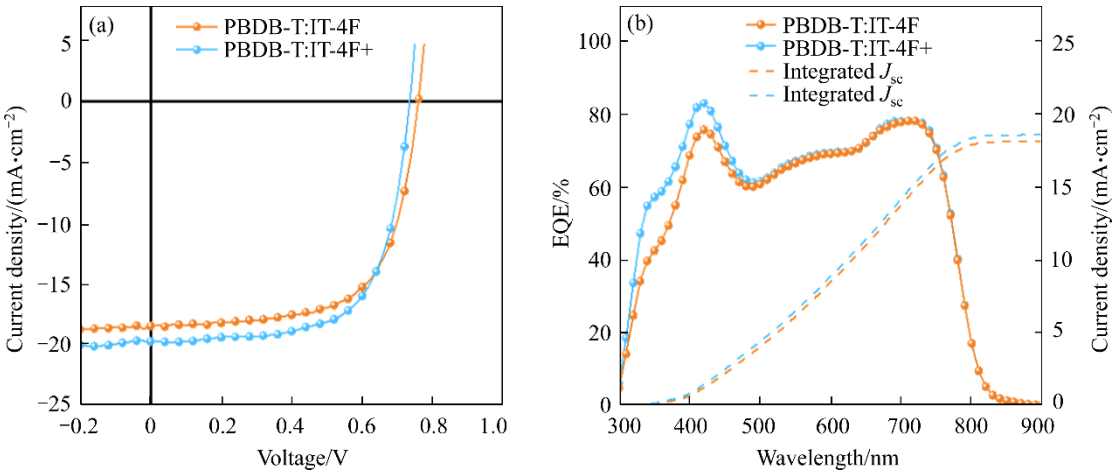


**Figure S3** *J*–*V* curves and EQE spectra of PBDB-T:IT-4F and PBDB-T:IT-4F+ based OSCs

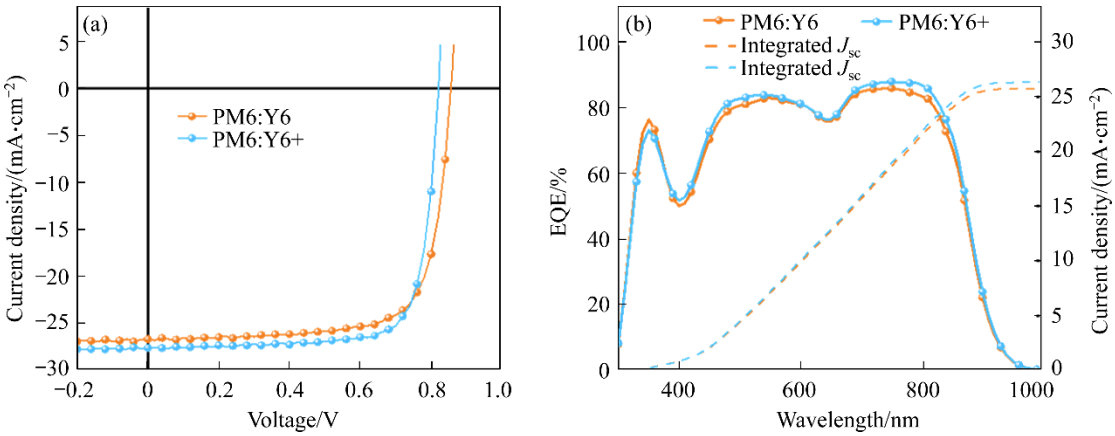


**Figure S4** *J*−*V* curves and EQE spectra of PM6:Y6 and PM6:Y6+ based OSCs

**Table S4** Photovoltaic parameters of OSCs based on PBDB-T:IT-4F, PBDB-T:IT-4F+, PM6:Y6 and PM6:Y6+ blend films

| Blend film | $V_{OC}$/V | $J_{SC}$/(mA·cm$^{-2}$) | FF/% | PCE/% | $J_{EQE}$/(mA·cm$^{-2}$) |
|---|---|---|---|---|---|
| PBDB-T:IT-4F | 0.759 (0.748±0.005) | 18.50 (18.47±0.39) | 65.17 (63.76±0.98) | 9.15 (8.80±0.17) | 18.12 |
| PBDB-T:IT-4F+ | 0.734 (0.732±0.003) | 19.72 (19.56±0.25) | 66.79 (66.29±0.75) | 9.67 (9.49±0.12) | 18.56 |
| PM6:Y6 | 0.856 (0.850±0.008) | 26.76 (26.61±0.31) | 74.33 (74.25±0.59) | 17.02 (16.80±0.19) | 25.75 |
| PM6:Y6+ | 0.821 (0.816±0.002) | 27.66 (27.44±0.25) | 77.95 (77.71±0.45) | 17.70 (17.40±0.17) | 26.35 |

Note: The average values and standard deviations of 10 devices are in parentheses.

## 8 Exciton dissociation

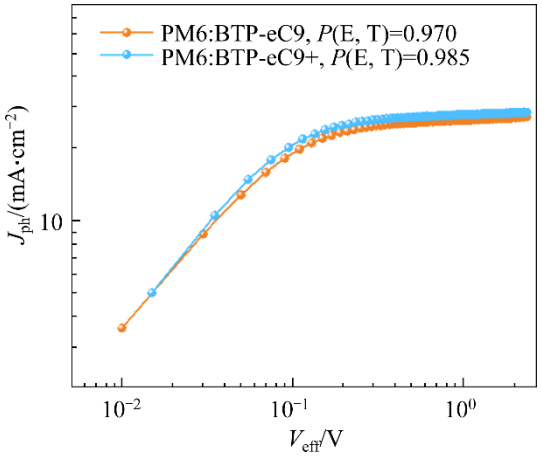


**Figure S5** Photocurrent density versus effective voltage curves of PM6:BTP-eC9 and PM6:BTP-eC9+ based OSCs

## 9 Monomolecular recombination

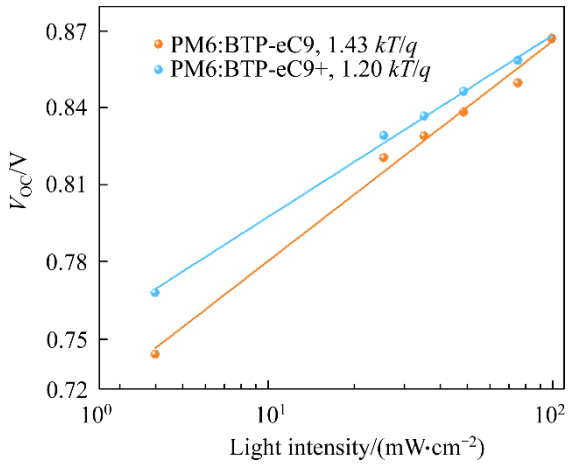


**Figure S6** Dependence of $V_{OC}$ on incident light intensity of PM6:BTP-eC9 and PM6:BTP-eC9+ based OSCs